(12) Glasstone, S., "An Introduction to Electrochemistry", 9th Printing, D. Van Nostrand, New York, N.Y., 1960, p 336.
(13) Gurney, R. W., *J. Chem. Phys.*, **6**, 499 (1938).
(14) Halban, H. v., Brüll, J., *Helv. Chim. Acta*, **27**, 1719 (1944).
(15) Halban, H. v., Ebert, L., *Z. Phys. Chem., Abt. A*, **112**, 321 (1924).
(16) Halban, H. v., Ebert, L., *Z. Phys. Chem., Abt. A*, **112**, 359 (1924).
(17) Halban, H. v., Eisenbrand, J., *Z. Phys. Chem., Abt. A*, **122**, 337 (1926).
(18) Halban, H. v., Eisenbrand, J., *Z. Phys. Chem., Abt. A*, **146**, 294 (1930).
(19) Halban, H. v., Siedentopf, K., *Z. Phys. Chem., Abt. A*, **100**, 208 (1922).
(20) Halban, H. v., Siedentopf, K., *Z. Phys. Chem., Abt. A*, **103**, 71 (1922).
(21) Harned, H. S., Owen, B. B., "The Physical Chemistry of Electrolytic Solutions", 3rd ed, Reinhold, New York, N.Y., 1958, pp. 651 and 456.
(22) Harned, H. S., Robinson, R. A., *Trans. Faraday Soc.*, **36**, 973 (1940).
(23) Ives, D. G. J., Janz, G. J., "Reference Electrodes", Academic Press, New York, N.Y., 1961, p 209.
(24) Latimer, W. M., Pitzer, K. S., Shansky, C. M., *J. Chem. Phys.*, **7**, 108 (1939).
(25) Meyer, E., Rosenberg, H., *Vierteljahresschr. Astron. Ges.*, **48**, 3 (1913).
(26) Morrision, R. T., Boyd, R. N., "Organic Chemistry", 2nd ed., Prentice-Hall of India, 1966, pp 600 and 579.
(27) Robinson, R. A., Stokes, R. H., "Electrolyte Solutions", 2nd ed, Butterworths, London, 1959, p 526.

Received for review July 5, 1977. Accepted December 20, 1977.

Enthalpies of Fusion, Freezing Points, Heat Capacities, Densities, and Shear Viscosities of Hydrogenated Dimers of Norbornadiene and Cyclopentadiene

Cornelius T. Moynihan,* Hiroyuki Sasabe, David S. Czaplak, and Urban E. Schnaus

Vitreous State Laboratory, Chemical Engineering and Materials Science Department, Catholic University of America, Washington, D.C. 20064

Enthalpies of fusion, freezing points, crystal and liquid heat capacities, liquid densities, and shear viscosities have been determined for four isomeric hydrogenated dimers of norbornadiene (NBD) and one hydrogenated cyclopentadiene dimer. The hydrogenated NBD dimers exhibit a large spread in their enthalpy of fusion values. The viscosities of the hydrogenated NBD dimers are all of comparable magnitude and considerably larger than the viscosity of the hydrogenated cyclopentadiene dimer. Relative magnitudes of the viscosities appear to be governed primarily by the T_2 parameter in the VTF equation.

Introduction

In this paper we report determinations of the freezing points, enthalpies of fusion, heat capacities, densities, and shear viscosities of high-purity specimens of four isomers of the hydrogenated dimers of norbornadiene (NBD) and of one lower molecular weight polycyclic alkane (*exo*-tetrahydrodicyclopentadiene). The structures of these compounds in terms of their carbon atom skeletons are shown in Figure 1, along with the abbreviations (HXX, etc.) by which they will be designated in the remainder of this paper.

Experimental Section

Samples of the five compounds of Figure 1 were obtained from Dr. A. Schneider of Suntech, Inc. Their purities, as determined by him using vapor-phase chromatography (VPC), are given in Table I. In all cases the impurities were other isomers of the same compound.

The heat capacity and melting behavior of these compounds were characterized using a Perkin-Elmer DSC-2 differential scanning calorimeter linked to a digital data acquisition system and cooled by a two-stage refrigerator when measurements were in the range −70 °C and above or by liquid N_2 when measurements at lower temperatures were required. The DSC temperature scale at each heating rate was calibrated using the melting points of Hg and H_2O. Samples were contained in sealed Al volatile sample pans. Sample masses ranged from 0.7 to 15.7 mg, smaller samples being used for enthalpy of fusion determinations and larger samples for crystal and liquid heat capacity determinations. Each sample was slowly cooled or held at a low temperature on the DSC until freezing occurred, as manifested by an exothermic signal on the DSC output. For enthalpy of fusion determinations the heat capacity C_p was then measured over the melting region while heating at a rate of 0.62 K/min. For crystal and liquid heat capacity determinations C_p was measured over a larger temperature interval at a heating rate of 5 or 10 K/min. Single-crystal Al_2O_3 and benzoic acid were used as heat capacity calibration standards. Temperature corrections during the fusion process necessitated by the thermal resistance between the sample pan and sample holder were made according to a previously described procedure (*11*).

Liquid kinematic viscosities ν were measured with factory calibrated Ubbelohde semimicrocapillary viscometers from the Cannon Instrument Co. Liquid densities ρ were measured with a dilatometer constructed by sealing off one end of a 1-mL pipet graduated in 0.01-mL divisions and calibrated by determining the mass of water needed to fill it to a reference mark. The shear viscosity η was obtained by taking the kinematic viscosity–density product $\nu\rho$. The viscometers and dilatometer were thermostated in a water bath (above 0 °C) or methanol bath (below 0 °C) contained in an unsilvered 4-qt Dewar flask. Bath temperatures were measured with a calibrated copper–constantan thermocouple. Viscosities and densities were measured from 70 or 75 °C down to either −69 °C or the temperature at which the sample froze; in the latter case this temperature was generally somewhat below the equilibrium freezing point due to supercooling of the sample. Shear viscosities are estimated to be accurate to about 1% above 0 °C and about 2% below 0 °C; the accuracy of the densities is estimated to be about 0.3%.

Results and Data Analysis

Equilibrium Freezing Point and Enthalpy of Fusion. In Figure 2 is shown a typical plot of heat capacity C_p vs. temperature T in the melting region. Integration of the excess heat capacity, $C_p^{\,x}$, above the baseline shown in Figure 2 gives the apparent specific enthalpy increase due to fusion as a function of the temperature:

$$\Delta h(T) = \int_{T' << T_0}^{T} C_p^{\,x} \, \mathrm{d}T' \qquad (1)$$

0021-9568/78/1723-0107$01.00/0

Table I. Molar Enthalpies of Fusion, ΔH_f, Pure Compound Melting Points, T_0, and Impurity mol %, $100(1-X)$

Compd	Formula	No. of determns	T_0, K	ΔH_f, kcal/mol	$100(1-X)$ By DSC	$100(1-X)$ By VPC
HXX	$C_{14}H_{18}$	3	285.3 ± 0.2	3.69 ± 0.05	2.7 ± 0.2	1.4
HXN	$C_{14}H_{18}$	4	294.1 ± 0.7	1.80 ± 0.08	1.7 ± 0.2	2.8
HNN	$C_{14}H_{18}$	3	281.0 ± 0.2	5.24 ± 0.30	1.5 ± 0.1	3.2
PXtX	$C_{14}H_{20}$	3	336.8 ± 0.6	2.89 ± 0.13	2.2 ± 0.3	0.8
XTHDCPD	$C_{10}H_{16}$	1	$182._4$	1.1_1	$3._2$	4

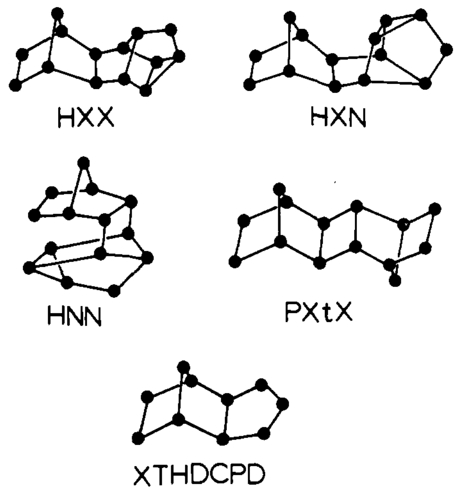

Figure 1. Structures of compounds studied in the present paper: hexacyclic *exo,exo*-dihydrodinorbornadiene (HXX), hexacyclic *endo,endo*-dihydrodinorbornadiene (HNN), hexacyclic *exo,endo*-dihydrodinorbornadiene (HXN), pentacyclic *exo-trans-exo*-tetrahydrodinorbornadiene (PXtX), *exo*-tetrahydrodicyclopentadiene (XTHDCPD).

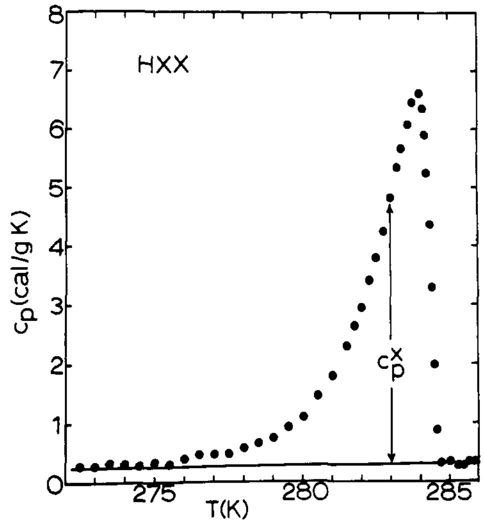

Figure 2. Heat capacity vs. temperature during fusion of a 1.24-mg sample of HXX while heating at 0.62 K/min.

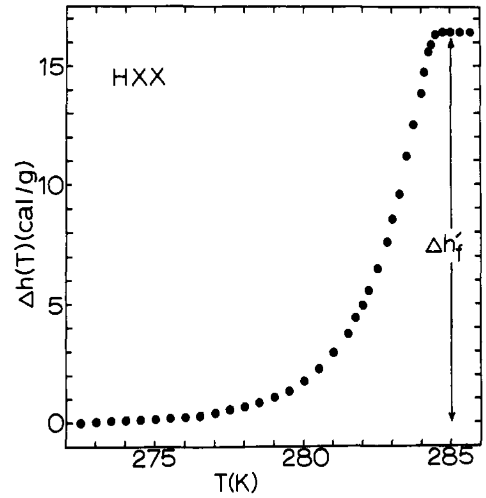

Figure 3. Apparent specific enthalpy increase due to fusion as a function of temperature for HXX obtained by integration of data in Figure 2.

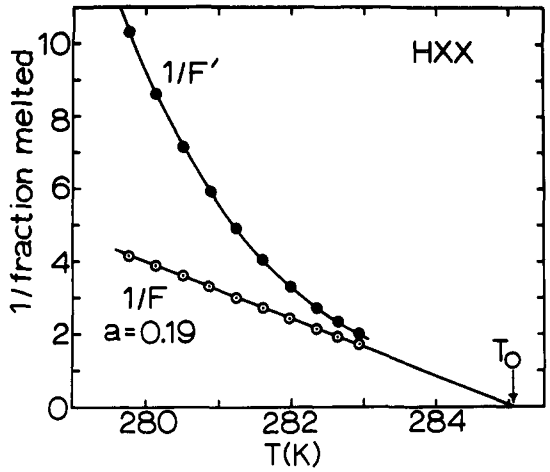

Figure 4. Plot vs. T of inverse of apparent fraction melted, $1/F'$, and corrected fraction melted, $1/F$, calculated using a correction factor of $a = 0.19$, for the HXX data of Figure 3.

where T_0 is the pure compound equilibrium melting point. A plot of $\Delta h(T)$ vs. T obtained from the data of Figure 2 is shown in Figure 3; the high-temperature limit of $\Delta h(T)$ is the apparent specific enthalpy of fusion, $\Delta h'_f$.

The sample of Figures 2 and 3 melts over a range in temperature because of the presence of impurities. The apparent fraction of the sample melted at a given temperature is defined as

$$F' = \Delta h(T)/\Delta h_f' \qquad (2)$$

Provided that there is no solid solution formation on freezing and that the mole fraction of impurities in the liquid is small enough that the liquid exhibits ideal solution behavior, then it may be shown that in the region near the pure compound melting point T_0 the temperature dependence of F' is given by (*7*, *9–12*)

$$\frac{1}{F'} = -\left[\frac{M\Delta h_f'}{(1-X)RT_0^2}\right](T - T_0) \qquad (3)$$

where M is the molecular weight, X the overall mole fraction of the principal component of the sample, and R the ideal gas constant. A plot of $1/F'$ vs. T should give a straight line from whose slope the sample purity X and from whose intercept with the T axis T_0 may be determined.

$1/F'$ determined from Figure 3 using, as recommended (*12*), the data between $F' = 0.1$ and $F' = 0.5$ is plotted vs. T in Figure 4; the plot is not linear. The explanation most frequently given (*10*, *12*) for this is that melting commences at the eutectic point, well below the observed fusion region, but in the early stages of melting the excess heat capacity C_p^x is too small to be discerned readily from the baseline heat capacity on the

Table II. Apparent and Corrected Specific Enthalpies of Fusion, $\Delta h_f'$ and Δh_f, Correction Factors, a, Pure Compound Melting Points, T_0, and Impurity mol %, $100(1-X)$, from Measurements on Four Samples of HXN

Sample mass, mg	$\Delta h_f'$, cal/g	a	Δh_f, cal/g	T_0, K	$100(1-X)$
1.13	6.7	0.38	9.3	294.6	1.6
1.29	8.3	0.245	10.3	294.6	2.0
1.32	7.7	0.225	9.4	294.2	1.5
10.83	8.6	0.13	9.7	293.1	1.8
Av	7.8 ± 0.8		9.7 ± 0.5	294.1 ± 0.7	1.7 ± 0.2

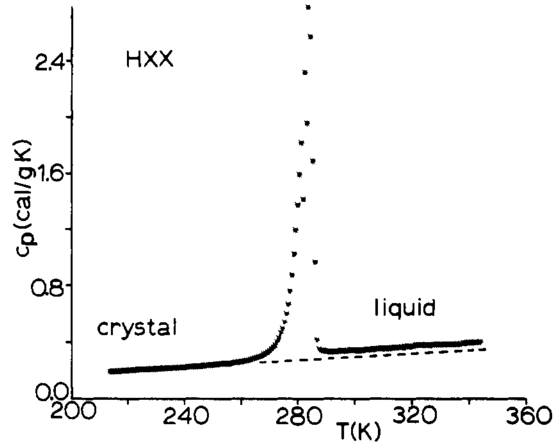

Figure 5. Heat capacity of a 15.72-mg sample of HXX measured at a heating rate of 5 K/min above and below the fusion region.

Table III. Parameters for Heat Capacity Equations $C_p(\text{cal/(g K)}) = C_p(T_0) + b[T(\text{K}) - T_0]$ for Crystals and Liquids[a]

Compd	No. of determns	T range, K	$C_p(T_0)$	b	Std dev C_p
HXX (cryst)	3	211–243	0.280	0.001 26	0.002
HXX (liq)		297–341	0.320	0.001 26	0.004
HXN (cryst)	3	208–261	0.297	0.001 05	0.008
HXN (liq)		326–344	0.340	0.001 05	0.002
HNN (cryst)	2	214–250	0.262	0.001 22	0.004
HNN (liq)		292–339	0.318	0.001 22	0.006
PXtX (cryst)	3	247–271	0.369	0.001 41	0.005
PXtX (liq)		344–384	0.381	0.001 41	0.005
XTHDCPD (liq)	5	210–340	0.254	0.000 88	0.009

[a] T_0 values are in Table I.

Table IV. Parameters for Liquid Density Equations $\rho(\text{g/cm}^3) = \rho(0) - b't(^\circ\text{C})$ and Molar Volumes, $\bar{V}$ at 70 °C

Compd	t range, °C	$\rho(0)$	$10^4 b'$	Std dev, ρ	$\bar{V}$, cm^3/mol
HXX	0 to 70	1.092	7.7	0.001	179.5
HXN	−8 to 70	1.092	7.9	0.001	179.7
HNN	−41 to 70	1.104	7.6	0.001	177.3
PXtX	65 to 75	1.038	(7.8)	0.002	191.5
XTHDCPD	−69 to 75	0.950	7.7	0.001	152.0

low-temperature side of the fusion peak. If one presumes that because of this the apparent enthalpy of fusion $\Delta h_f'$ underestimates the true enthalpy of fusion by a factor $(1 + a)$, then one may define corrected values of the specific enthalpy of fusion and fraction melted

$$\Delta h_f = (1 + a)\Delta h_f' \tag{4}$$

$$F = (\Delta h(T) + a\Delta h_f')/(1 + a)\Delta h_f' \tag{5}$$

and eq 3 becomes

$$\frac{1}{F} = -\left[\frac{M\Delta h_f}{(1-X)RT_0^2}\right](T - T_0) \tag{6}$$

$1/F$ is also plotted vs. T in Figure 4, where the correction factor a has been selected by a computer fit to linearize the plot.

In Table II are listed values of $\Delta h_f'$, a, Δh_f, T_0, and $100(1 - X)$ (the latter two quantities calculated from eq 6) obtained from measurements on four separate samples of the HXN compound. The value of the correction factor a varies widely for the different samples, but the use of the appropriate a value for each determination leads to good agreement among the Δh_f values as compared to that among the $\Delta h_f'$ values and—a more sensitive criterion of self-consistency of results by this method—to good agreement among the calculated values of $100(1 - X)$.

In Table I are listed the corrected molar enthalpy of fusion ΔH_f $(= M\Delta h_f)$, T_0, and $100(1 - X)$ for each of the five compounds studied here. For the NBD hydrogenated dimers the values are averages of results obtained for three or four separate samples of a given compound. Due to the low temperature the DSC output during fusion of the XTHDCPD was quite noisy, and the ΔH_f value quoted for this compound is probably accurate to within only 10–20%.

Crystal and Liquid Heat Capacities. In Figure 5 are shown the results of a typical DSC scan used to determine crystal and liquid heat capacities. For the hydrogenated NBD dimers, within experimental error the crystal heat capacities below the fusion region and the liquid heat capacities above the fusion region were both linear functions of temperature with identical temperature dependences. For XTHDCPD only the liquid heat capacity was measured. Respective crystal and liquid C_p results from two to five determinations were combined and fitted to equations of the form

$$C_p(\text{cal/(g K)}) = C_p(T_0) + b[T(\text{K}) - T_0] \tag{7}$$

where $C_p(T_0)$ is the heat capacity at the pure compound freezing point T_0 (cf. Table I). For these compounds the constraint was imposed that the crystal C_p data be fit with the slope b obtained from a least-squares fit to the C_p data for the corresponding liquid. Parameters for eq 7 are given in Table III.

Liquid Densities. Within experimental error the liquid densities were linear functions of temperature and were least-squares fitted to equations of the form

$$\rho(\text{g/cm}^3) = \rho(0) - b't(^\circ\text{C}) \tag{8}$$

where $\rho(0)$ is the density at 0 °C. Parameters for eq 8 for the five compounds are given in Table IV, along with the molar volumes $\bar{V}(=M/\rho)$ at 70 °C. The short temperature range over which density data were obtained for PXtX made a meaningful fit to eq 8 impossible. Hence the b' parameter for PXtX was arbitrarily set equal to roughly the mean of the b' values for the other liquids and the corresponding $\rho(0)$ value calculated from the density data.

Shear Viscosities. The temperature dependences of liquid shear viscosities are shown in the form of an Arrhenius plot (log η vs. $10^3/T(\text{K})$) in Figure 6 for two of the compounds. As is common for organic liquids in this viscosity range (*2*, *4*, *5*) the plots are curved and concave upward, but may be well described by the semiempirical Vogel–Tammann–Fulcher (VTF) equation:

$$\ln \eta(P) = A + \frac{B}{T(\text{K}) - T_2} \tag{9}$$

where A, B, and T_2 are constants. The solid lines in Figure 6 are computer fits of the data to eq 9 obtained using a previously described procedure (*8*). The VTF equation parameters for the five compounds are given in Table V. For the PXtX compound, again because of the short temperature range over which data were obtained, the T_2 parameter was arbitrarily set

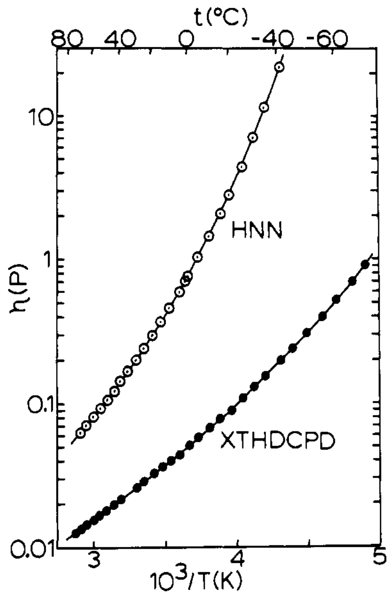

Figure 6. Arrhenius plots of shear viscosities of HNN and XTHDCPD. Solid lines are calculated using least-squares VTF equation parameters.

Table V. Parameters for the VTF Equation for Shear Viscosity, $\ln \eta(\mathrm{P}) = A + B/(T(\mathrm{K}) - T_2)$

Compd	t range, °C	A	B	T_2	Std dev $\ln \eta$
HXX	0 to 70	−6.925	698.2	162.0	0.001
HXN	−5 to 70	−7.411	867.9	151.0	0.007
HNN	−41 to 70	−7.191	866.0	148.0	0.006
PXtX	65 to 75	−7.526	854.4	(150.0)	0.002
XTHDCPD	−69 to 75	−7.634	836.3	93.0	0.010

equal to a value in the range of the T_2 values of the other hydrogenated NBD dimers and the corresponding A and B parameters calculated from the viscosity data. It has been found experimentally for organic liquids that the Arrhenius plot tends to straighten out at low temperatures and VTF equation parameters obtained from a fit to data in the viscosity range measured in the present study tend to overestimate viscosities when extrapolated to lower temperatures (*2*, *4*, *5*). Hence caution should be employed in using the VTF equation parameters of Table V to extrapolate much beyond the temperature range covered by the actual data.

Discussion

The most dramatic differences in the properties of the four hydrogenated NBD dimers studied here occur in the molar enthalpies of fusion, ΔH_f, and molar entropies of fusion, ΔS_f ($=\Delta H_f/T_0$). There is no obvious correlation between molecular structure (Figure 1) and ΔH_f of these compounds. It sometimes happens that a compound will exhibit an unusually low heat of fusion (and an unusually high melting point) because of the occurrence of crystal–crystal phase transitions below the melting point. These impart some liquid-like degrees of freedom to the high-temperature crystalline form and "use up" part of the enthalpy change that would occur on fusion in the absence of such crystal–crystal transitions. No such transitions, which would give rise to endothermic DSC peaks, were observed for the hydrogenated NBD dimer crystals in the range 200 K up to their melting points. On the other hand the DSC scan of the XTHDCPD at 10 K/min revealed a crystal–crystal transition in the temperature range 145–150 K.

The values of the impurity mol %, $100(1 - X)$, for the five compounds obtained by DSC and by VPC are not in particularly good agreement compared to the precision of the DSC results, but there is no consistent pattern in the discrepancies, i.e., in some cases the DSC result is higher and in other cases the VPC result is higher. The discrepancies may be due in part to the difficulty in estimating accurately the areas under the several small impurity peaks in the vapor-phase chromatograms.

Table VI. Comparison of Shear Viscosities η (P) and Viscosity Activation Enthalpies Δh^* (kcal/mol) at Different Temperatures

Compd	t, °C: −40	0	30	70
HXX η		0.526	0.138	0.0464
Δh^*		8.4	6.4	5.0
HXN η		0.737	0.181	0.0553
Δh^*		8.6	6.8	5.5
HNN η	19.7	0.762	0.200	0.0637
Δh^*	12.9	8.2	6.6	5.3
PXtX η				0.0449
Δh^*				5.4
XTHDCPD η	0.188	0.0501	0.0259	0.0137
Δh^*	4.6	3.8	3.5	3.1

At a given temperature the heat capacities of the four hydrogenated NBD dimer crystals are all very nearly equal; the same is true of the liquid heat capacities. For example, the mean of the crystal heat capacities at 250 K is 0.240 ± 0.012 cal/(g K), while the mean of the liquid heat capacities at 340 K is 0.388 ± 0.002 cal/(g K). The 340 K liquid C_p for XTHDCPD, 0.393 cal/(g K), is quite close to that for the NBD hydrogenated dimers.

The five compounds studied here all have virtually identical temperature dependences ($d\rho/dt = -b'$) of their densities. The molar volumes $\bar{V}$ at 70 °C given in Table IV fall in the order (PXtX > HXX ≈ HXN > HNN > XTHDCPD) one would expect from the structures of Figure 1 on the basis of molecular size and compactness.

In Table VI the shear viscosities (calculated using the parameters of Table V) and the activation enthalpies

$$\Delta h^* \equiv R(\mathrm{d} \ln \eta/\mathrm{d}(1/T)) = RBT^2/(T - T_2)^2 \qquad (10)$$

are compared for the five compounds at various temperatures. The temperature dependences, i.e., Δh^* values, of the NBD hydrogenated dimer viscosities are all virtually identical at a given temperature. The viscosities of the NBD hydrogenated dimers at a given temperature are also quite similar, but there does appear to be something of a trend in the viscosities (HNN > HXN > HXX > PXtX) in the direction of decreasing viscosity with decreasing molecular compactness (cf. Figure 1). At a given temperature η and Δh^* of the lower molecular weight hydrocarbon XTHDCPD are considerably less than the corresponding values for the NBD hydrogenated dimers.

The T_2 parameter in eq 9 is the temperature at which the shear viscosity of the liquid would become infinite, provided that the VTF equation described the viscosity temperature dependence accurately at all temperatures. T_2 has been interpreted theoretically as the temperature at which the free volume (*3*, *4*) or the configurational entropy (*1*) of the liquid vanishes. Lewis (*6*) has found that the T_2 parameter for *n*-alkanes increases with increasing molecular weight. Hence it is not unexpected that the hydrogenated NBD dimers all exhibit T_2 values fairly close to one another and considerably larger than the T_2 value for the lower molecular weight XTHDCPD. It is also worth noting that, in terms of the VTF equation parameters, it is the difference between the T_2's of the hydrogenated NBD dimers and the T_2 for XTHDCPD that is primarily responsible for the lower viscosity and Δh^* of the XTHDCPD with respect to the other compounds, i.e., the respective A and B parameters in Table V are all of comparable magnitude for the five compounds.

Acknowledgment

The authors wish to thank Dr. A. Schneider for providing samples of the compounds studied here, which were prepared

as part of an Air Force/Navy sponsored program.

Literature Cited

(1) Adams, G., Gibbs, J. H., *J. Chem. Phys.*, **43**, 139 (1965).
(2) Barlow, A. J., Lamb, J., Matheson, A. J., *Proc. R. Soc. London, Ser. A*, **292**, 322 (1966).
(3) Cohen, M. H., Turnbull, D., *J. Chem. Phys.*, **31**, 1164 (1959).
(4) Cukierman, M., Lane, J. W., Uhlmann, D. R., *J. Chem. Phys.*, **59**, 3639 (1973).
(5) Laughlin, W. T., Uhlmann, D. R., *J. Phys. Chem.*, **76**, 2317 (1972).
(6) Lewis, O. G., *J. Chem. Phys.*, **43**, 2693 (1965).
(7) Marti, E. E., *Thermochim. Acta*, **5**, 173 (1972).
(8) Moynihan, C. T., *J. Phys. Chem.*, **70**, 3399 (1966).
(9) Plato, C., Glasgow, A. R., Jr., *Anal. Chem.*, **41**, 330 (1969).
(10) Sondack, D. L., *Anal. Chem.*, **44**, 888 (1972).
(11) Thermal Analysis Newsletter, No. 5, Perkin-Elmer Corp., Norwalk, Conn.
(12) Thermal Analysis Newsletter, No. 6, Perkin-Elmer Corp., Norwalk, Conn.

Received for review July 26, 1977. Accepted November 9, 1977. This research was supported by Contract No. N00019-76-C-0166 from the Naval Air Systems Command.

Enthalpies of Combustion of 1,1,4,4-Tetramethylcyclodecane and of 1,1,5,5-Tetramethylcyclodecane in the Liquid State

Harm Dekker and Cornelis Mosselman*

Laboratory of Physical Chemistry, the Free University, De Boelelaan 1083, Amsterdam, The Netherlands

Enthalpies of combustion of 1,1,4,4-tetramethylcyclodecane and of 1,1,5,5-tetramethylcyclodecane in the liquid state have been determined. For the 1,1,4,4 compound $-\Delta H_c^\circ$(l, 298.15 K)/kJ mol^{-1} = 9172.7 ± 1.2 and for the 1,1,5,5 compound $-\Delta H_c^\circ$(l, 298.15 K)/kJ mol^{-1} = 9182.2 ± 1.7. The difference between the enthalpies of combustion is 9.5 ± 1.4 kJ mol^{-1}. A possible correction of about +0.02% to be applied to $-\Delta H_c^\circ$, connected with the presence of dissolved air in the samples, is discussed. The densities, required for buoyancy corrections, were determined.

Introduction

In this article is described the combustion-calorimetric part of the study by Bixon, Dekker, Dunitz, Eser, Lifson, Mosselman, Sicher, and Svoboda (*4*) about structural and strain-energy consequences of "intraannular" substitution in the cyclodecane ring. The samples of 1,1,4,4-tetramethylcyclodecane and of 1,1,5,5-tetramethylcyclodecane were provided by Svoboda, Yudin, and Sicher. The syntheses, purification, and purity control have been described (*16*).

Experimental Section

Apparatus. The temperature of the isoperibol combustion bomb calorimeter (*6–8*, *13*) was measured with the platinum resistance thermometer and the Smith method No. 3 bridge described in ref 13.

The calorimeter was calibrated with benzoic acid, National Bureau of Standards sample 39i, certified to have a specific internal energy of combustion of 26434 J g^{-1} under so-called certification conditions (*12*).

The method of enclosing the volatile sample was the version of the covered crucible method (*14*) that has been indicated in footnote *a* of that reference.

For particulars concerning the balance for weighing the sample and concerning ancillary equipment for the resistance measurements, see ref 13. To ensure the constancy of the amount of water in the calorimeter can (apart from a buoyancy correction, ref 13) within a series of combustions, a balance was used having a reproductibility of 50 mg at a maximum load of 5 kg per pan.

Materials. The oxygen used in the combustion bomb was first passed through a purifier (*1*), designed for the removal of oxidizable impurities, as a matter of routine.

The organic impurity content of the samples to be burned was less than 0.05% (*16*).

Procedure. This was essentially as described in ref 13. The sample was ignited when the calorimeter temperature had reached 25.00 °C. The amount of sample was chosen so that a final temperature of 27 °C was obtained. The jacket temperature was about 26.0 °C, with a stability of about ±0.001 °C. Variations were accounted for (*12*). The initial and the final rating period were 4 and 8 min, respectively. In the least-squares method, both periods were approximated as straight lines (*12*). The reaction period was taken as only 11.5 min in order to speed up the experiment. This duration is somewhat too short for the thermal equilibration to be complete, but the error arising from this fact, in the order of 0.01%, is the same in a calibration with benzoic acid, and, therefore, cancels.

Units and Auxiliary Quantities. Throughout this section, 1 bar = 10^5N m^{-2}. In the bomb was placed 1 cm^3 of water and the bomb was flushed with oxygen in order to remove the air from its interior (*9*). The bomb was charged with oxygen to a pressure of 30.9 bar at 25.00 °C. The volume of the bomb available to the reactants and the water was 0.3360 dm^3.

For the combustible auxiliary substances we measured and used the following values valid at 25.00 °C: Vaseline, $-\Delta u_c^\circ$/J g^{-1} = 45997.8 ± 2.8; cotton thread used as the fuse, $-\Delta u_c^\circ$/J g^{-1} = 16470. Δu_c° is the change in internal energy upon combustion, with the reactants and the products in their standard states. The uncertainty interval represents twice the standard deviation of the mean of the series of combustions. The elemental composition of the Vaseline was $C_1H_{1.888}$ and its density 0.854 g cm^{-3}.

The water content of the samples was determined by means of the Karl Fischer dead-stop method (*2*). The 1,1,4,4 compound and the 1,1,5,5 compound were found to have a water content of 0.008 ± 0.002% and of 0.011 ± 0.004%, respectively. The uncertainties given are estimated maximum uncertainties.

The samples as weighed were saturated with air. Because of uncertainty as regards the exact value of the correction, for this aspect, to be applied to the weighed masses, enthalpies of combustion are given at this stage as calculated from the uncorrected mass. The correction to ΔH_c°(l) should be about 0.02–0.03%; see for instance ref 3.

The vapor pressure of the substances was low enough to allow one to neglect, in the buoyancy correction of weighed masses, the presence of vapor in the gas space of the closed crucible.

The values of the densities of the samples, used to calculate the buoyancy correction and reduction to standard states (*10*),